

1       **Renal hemodynamics and fatty acid uptake: effects of obesity and**  
2   **weight loss**

3  
4       **Eleni Rebelos<sup>1</sup>, Prince Dadson<sup>1</sup>, Vesa Oikonen<sup>2</sup>, Hidehiro Iida<sup>1</sup>, Jarna C. Hannukainen<sup>1</sup>,**  
5   **Patricia Iozzo<sup>1,3</sup>, Ele Ferrannini<sup>\*3</sup>, Pirjo Nuutila<sup>\*1,4</sup>**

6  
7   **\* equal contribution**

8  
9       <sup>1</sup>**Turku PET Centre, University of Turku, Turku, Finland**

10      <sup>2</sup>**Turku PET Centre, Turku University Hospital, Turku, Finland**

11      <sup>3</sup>**Institute of Clinical Physiology, National Research Council (CNR), Pisa, Italy**

12      <sup>4</sup>**Department of Endocrinology, Turku University Hospital, Turku, Finland**

13  
14   Running title: Free fatty acids and renal metabolism

15  
16      Corresponding author: Pirjo Nuutila, Turku PET Centre, University of Turku, and Department of  
17      Endocrinology, Turku University Hospital, Turku, Finland. Tel: 0358/23131868; E-mail:  
18      pirjo.nuutila@utu.fi

19  
20      Word Count Abstract: 238

21      Word Count Main Text: 3423

22      Number of References: 40

23      Number of Tables: 3

24      Number of Figures: 4

25

## 26 Abstract

27

28 Human studies of renal hemodynamics and metabolism in obesity are insufficient. We  
29 hypothesized that renal perfusion and renal FFA uptake are higher in morbidly obese as compared  
30 to lean subjects and that they both decrease after bariatric surgery. Cortical and medullary  
31 hemodynamics and metabolism were measured in 23 morbidly obese women and 15 age- and sex-  
32 matched nonobese controls by PET scanning of [ $^{15}\text{O}$ ]- $\text{H}_2\text{O}$  (perfusion) and 14(*R, S*)-[ $^{18}\text{F}$ ]fluoro-6-  
33 thia-heptadecanoate (free fatty acid [FFA] uptake). Kidney volume and radiodensity were  
34 measured by CT, cardiac output by MRI. Obese subjects were re-studied 6 months after bariatric  
35 surgery.

36 Obese subjects had higher renal volume but lower radiodensity, suggesting accumulation of water  
37 and/or lipid. Both cardiac output and glomerular filtration rate (eGFR) were increased by ~25% in  
38 the obese. Total renal blood flow was higher in the obese (885 [317] vs 749 [300] ml/min of  
39 controls,  $p=0.049$ ). In both groups, regional blood perfusion was higher in the cortex than medulla;  
40 in either region, FFA uptake was ~50% higher in the obese as a consequence of higher circulating  
41 FFA levels. Following weight loss ( $26\pm 8$  kg), total renal blood flow was reduced ( $p=0.006$ ). Renal  
42 volume, eGFR, cortical and medullary FFA uptake were decreased but not fully normalized.  
43 Obesity is associated with renal structural, hemodynamic, and metabolic changes. Six months after  
44 bariatric surgery, the hemodynamic changes are reversed, and the structural changes are improved.  
45 On the contrary, renal FFA uptake remains increased, driven by high substrate availability.

46

47 Keywords: PET, obesity, bariatric surgery, free fatty acids, renal hemodynamics

48 Abbreviations: BMI: body mass index; BSA: body surface area; Chronic Kidney Disease  
49 Epidemiology Collaboration: CKD-EPI; CT: computerized tomography; FFA: free-fatty acids;  
50 FOV: field of view; FTHA: 14(*R, S*)-[ $^{18}\text{F}$ ]fluoro-6-thia-heptadecanoic acid; FUR: fractional uptake  
51 rate; Glomerular filtration rate: GFR; HU: Hounsfield units; MRI: Magnetic resonance imaging;  
52 OGIS: oral glucose insulin sensitivity; OGTT: oral glucose tolerance test; PET: positron emission  
53 tomography; RFAU: renal fatty acid uptake; ROI: region of interest; RYGB: Roux-en-Y gastric  
54 bypass; SGLT2: sodium glucose cotransporter 2; T2D: type 2 diabetes; WHP: waist-to-hip ratio

55

56

## 57 Introduction

58

59 The incidence of obesity is on the rise virtually worldwide (40). While diabetes and  
60 hypertension are the two most common risk factors for the development of chronic kidney disease  
61 (CKD) (12), mounting evidence indicates that obesity *per se* poses an additional risk (39). Human  
62 studies of the renal hemodynamics and metabolism in obesity are scanty, however, in part due to the

63 difficulty of accounting for the heteromorphism of renal cell types and the diversity in perfusion  
64 and function in different renal regions (35).

65 The kidney is a richly perfused organ, receiving approximately 20% of cardiac output, and has  
66 a unique perfusion system. Blood supply to the renal cortex occurs through the afferent arterioles  
67 of each nephron while blood supply to the medulla occurs only through the vasa recta of the  
68 juxtaglomerular nephrons. It follows that perfusion in the renal cortex is higher than in the medulla.  
69 This high cortical perfusion serves for the filtration of large volumes of blood through the glomeruli  
70 as well as the reabsorption of proteins, substrates and electrolytes; the main function of the medulla  
71 is the active reabsorption of water and solutes.

72 The energy for these processes is provided by very active metabolic processes. Tubular cells in  
73 the cortex, such as those in proximal tubules and the thick ascending limb of the loop of Henle, are  
74 rich in mitochondria and depend predominantly on oxidative metabolism, with fatty acids, ketone  
75 bodies, and lactate being the preferred substrates (2). On the other hand, cells in the inner medulla,  
76 such as those of the thin descending and ascending limbs of the loop of Henle and the collecting  
77 duct, have few mitochondria and depend predominantly on glycolysis for energy production (26).  
78 The renal cortex also contributes to gluconeogenesis (28); renal gluconeogenesis is confined to the  
79 proximal tubule since the key enzymes in the pathway – glucose-6-phosphatase, fructose-1,6-  
80 biphosphatase, and phosphoenolpyruvate carboxykinase – are only found there (33).

81 Regulation of renal hemodynamics is primarily achieved by changes in arteriolar resistance,  
82 which can jointly affect both renal blood flow and glomerular filtration rate (GFR) (32). However,  
83 some basic aspects regarding the interplay between renal perfusion and cardiac output have not  
84 been clarified. Thus, cardiac output is increased in obese subjects (19) and decreases after weight  
85 loss (24). However, it is not known how these changes affect renal perfusion and metabolism.  
86 Therefore, aims of the present study were to simultaneously measure regional, *i.e.*, cortical *vs*  
87 medullary, hemodynamics and metabolism *in vivo* in obese subjects – with or without type 2  
88 diabetes (T2D) – and nonobese controls, and to determine the effects of major weight loss. As free  
89 fatty acids (FFA) are the main substrate for the kidney in the fasting state, we employed positron-  
90 emitting tomography (PET) to quantitate both perfusion (with the use of  $^{15}\text{O}$ -labelled water) and  
91 FFA uptake (using the long-chain fatty acid analog 14(*R,S*)- $^{18}\text{F}$ fluoro-6-thia-heptadecanoic acid  
92 ( $^{18}\text{F}$ -FTHA)).

93

## 94 **Methods**

95

96 *Participants and study design* We studied 23 morbidly obese women and 15 age- and sex-  
97 matched healthy nonobese controls. Obese patients were studied before and 6 months after bariatric  
98 surgery, and controls were studied only once along with the patients. Inclusion and exclusion  
99 criteria have been described in detail (13). Based on ADA criteria (1), 10 obese patients had type 2  
100 diabetes (T2D) and 13 were nondiabetic (ND), including 4 with impaired glucose tolerance and 1  
101 with impaired fasting glucose before the operation. Nine of the obese subjects had a diagnosis of  
102 arterial hypertension. Eight obese were treated with laparoscopic Roux-en-Y gastric bypass  
103 (RYGB) and 15 with laparoscopic sleeve gastrectomy. Data on adipose tissue (4) and liver (16)  
104 fatty acid uptake from these subjects have been previously reported. The protocol was approved by  
105 the Ethics Committee of the Hospital District of Southwestern Finland, and all subjects gave written  
106 informed consent before participating in the study (NCT01373892).

107 *Study protocol* Clinical screening, anthropometric and biochemical measurements were  
108 performed as described (14). Blood pressure was measured with OMRON 711 automatic blood  
109 pressure monitor (Omron Corporate, Kyoto, Japan). Subjects then underwent positron-emitting  
110 tomography/computerized tomography (PET/CT) measurements in the fasting state using a hybrid  
111 GE discovery STE and VCT scanners (General Electric Medical Systems, Milwaukee, WI, USA).  
112 In obese patients, the imaging studies were performed before the standard 4-week very-low calorie  
113 diet that preceded surgery. For the PET studies, 2 catheters were inserted in the antecubital veins,  
114 one for the administration of radiolabeled tracers and the other for arterialized blood sampling.  
115 Subjects underwent CT scans that served as attenuation map and as anatomical reference for PET  
116 images. Subjects were injected with an intravenous bolus ( $554 \pm 124$  Mbq) of  $^{15}\text{O}$ -labelled water  
117 ( $^{15}\text{O}$ -H<sub>2</sub>O) followed by dynamic PET acquisition in the abdominal region (26 frames  $\times$  310 s).  
118 After 10 min, study subjects were given an intravenous bolus ( $185 \pm 46$  MBq) injection of [ $^{18}\text{F}$ ]-  
119 FTHA, following which the dynamic PET imaging of thoracic and upper body regions started (4,  
120 16). After  $86 \pm 3$  min, the abdomen was scanned (5 frames  $\times$  180 s) (14). Blood samples were  
121 drawn during the entire scanning period to measure FFA as well as radioactivity levels.

122 *Radiotracers* The production of [ $^{15}\text{O}$ ]-H<sub>2</sub>O ( $t_{1/2} = 122$  s) (10) and [ $^{18}\text{F}$ ]-FTHA ( $t_{1/2} = 110$  min)  
123 (15) have been described previously.

124 *PET data analysis* PET images were reconstructed in 256  $\times$  256 matrix after correction for  
125 decay time, dead time, and photon attenuation. Image analysis was performed using Carimas v.2.9  
126 (<http://www.turkupetcentre.fi/>). To obtain the time-radioactivity curves, the regions of interest  
127 (ROIs) were manually drawn on PET/CT fusion images in renal cortex and medulla (**Figure**  
128 **1A&1B**). In particular, consecutive thin ROIs were drawn in the renal cortex while avoiding tissue  
129 borders in 4-5 consecutive planes on both kidneys for [ $^{18}\text{F}$ ]-FTHA, and in 10-12 consecutive planes

130 in each kidney for [ $^{15}\text{O}$ ]- $\text{H}_2\text{O}$ , due to larger inhomogeneity in the signal. A second thin ROI was  
131 drawn more centrally on the same slices, representing the medulla.

132 Renal blood flow was calculated from radiowater PET scans using a one-tissue compartmental  
133 model, as previously described by Inaba *et al.* (17) and Kudomi *et al.* (22). The image-derived  
134 input function from abdominal aorta was used in the calculation (14). Glomerular filtration rate  
135 (eGFR, in  $\text{mL}/\text{min}/1.73\text{m}^2$ ) was estimated by the Chronic Kidney Disease Epidemiology  
136 Collaboration (CKD-EPI) equation (23). eGFR in  $\text{mL}/\text{min}$  was obtained using the individual values  
137 of body surface area (BSA) calculated according to Du Bois and Du Bois (6).

138 For the calculation of FFA uptake (FAU) from [ $^{18}\text{F}$ ]-FTHA-PET acquisitions, metabolite  
139 correction was performed for the radioactivity curves on the assumption that any residual activity  
140 after 30 min is attributable to metabolites. Plasma and tissue time-radioactivity curves were  
141 analyzed graphically using the linearization method (29). The slope of the plot in the graphical  
142 analysis equals the fractional uptake rate (FUR) of [ $^{18}\text{F}$ ]-FTHA. FUR values were corrected for  
143 renal tissue density ( $1.05 \text{ kg L}^{-1}$ ), and multiplied by the serum FFA concentration ( $\mu\text{mol}/\text{L}$ ) during  
144 the [ $^{18}\text{F}$ ]-FTHA-PET scanning to obtain the tissue FAU ( $\mu\text{mol min}^{-1} \cdot 100\text{g}^{-1}$ ).

145 *Renal volume and tissue density* Renal volume was measured using CT. Magnetic resonance  
146 imaging (MRI) was also used for those subjects in whom neither kidney was in the field of view in  
147 the CT. A 2-D mask was applied to all slices of each kidney thus creating a 3-D estimate of renal  
148 volume. The renal pelvis was excluded from the images. The final volume was obtained after  
149 visual inspection of each slice in order to fine-tune the voxels that would be part of the renal mask  
150 (**Figure 1C**). In all subjects, tissue radiodensity in Hounsfield units (HU) was also obtained. The  
151 analysis of images was performed using Carimas v.2.9 (<http://www.turkupetcentre.fi/>).

152 *Measurement of cardiac output* Cardiac output was measured by MRI as previously described  
153 (20).

154 *Indirect calorimetry* Open-system indirect calorimetry (Deltatrac®) was used for the  
155 measurement of  $\text{O}_2$  consumption ( $\text{VO}_2$ ) and  $\text{CO}_2$  production ( $\text{VCO}_2$ ), from which whole-body  
156 energy expenditure, and substrate oxidation rates were calculated as previously described (34).

157 *Selected metabolites* Selected plasma metabolites were measured by nuclear magnetic  
158 resonance spectroscopy, as previously described (36).

159 *Calculations and statistical analysis* Insulin sensitivity was estimated by the OGIS (Oral  
160 Glucose Insulin Sensitivity) method (25). On the assumption that cortical renal blood flow  
161 represents the near totality of blood flow to the kidney, total renal blood flow was obtained as the  
162 product of cortical blood perfusion and renal volume. The filtration fraction was calculated as the  
163 ratio of eGFR to total renal plasma flow.

164 Continuous variables are expressed as mean  $\pm$  SD. The normality of distribution was assessed  
165 using the Shapiro-Wilkinson test; variables that were not normally distributed were logarithmically  
166 transformed before analysis. One-way analysis of variance (ANOVA) was used to compare control  
167 subjects with obese patients, and nondiabetic with T2D subjects at baseline. The effect of surgery  
168 was tested by Wilcoxon signed rank test. Two-way ANOVA for repeated measures was used to  
169 compare the data of nondiabetic and T2D subjects before and after surgery. Pearson's correlation  
170 coefficient was used to investigate associations between body composition and renal metabolism.  
171 Statistical analysis was performed using JMP; significance was set at  $p \leq 0.05$ .

172

## 173 Results

174

175 *Clinical and metabolic characteristics (Table 1)* The patients with T2D ( $n = 10$ ) were matched  
176 to the nondiabetic obese participants ( $n = 13$ ) by age ( $45 \pm 7$  vs  $41 \pm 11$  years,  $p = \text{ns}$ ) and BMI ( $40.4$   
177  $\pm 4.6$  vs  $41.7 \pm 4.0$  kg/m<sup>2</sup>,  $p = \text{ns}$ ), and were in good glycemic control ( $\text{HbA}_{1c} = 6.4 \pm 0.7\%$ , fasting  
178 plasma glucose =  $6.4 \pm 1.0$  mmol/L). Except for  $\text{HbA}_{1c}$  and fasting glucose, none of the parameters  
179 measured in the obese participants in this study differed by T2D either before or after surgery; the  
180 data of nondiabetic and T2D participants were therefore pooled for further analysis.

181 As expected, obese participants had higher waist-to-hip ratio (WHR), fat mass, plasma FFA  
182 and glycerol concentrations as compared to controls, while eGFR (per 1.73 m<sup>2</sup> of body surface area)  
183 was similar.

184 *Hemodynamics* Cardiac output was increased by  $\sim 25\%$  in the obese group as were  $\text{VO}_2$ ,  
185  $\text{VCO}_2$ , and energy expenditure (Table 2). In the pooled baseline data, all these parameters were  
186 strongly related to the BMI (or other measures of body size, such as body weight, body surface area,  
187 and lean body mass), such that differences between obese and control participants were no longer  
188 statistically significant when adjusted for BMI.

189 In the kidney, cortical perfusion (per unit tissue volume) was significantly higher as compared  
190 to medullary perfusion ( $p < 0.0001$ ) in both obese and controls. Cortical and medullary blood  
191 perfusion rates (per unit tissue volume) were not different between the two groups.

192 • The total volume (both kidneys) was higher in the obese, but the radiodensity index (HU)  
193 was lower, indicating an increased content of water or lipid (or both) in the obese. By  
194 attributing the cortical blood perfusion to the entire measured volume, renal blood flow  
195 was higher ( $p = 0.049$ ) in obese than lean participants. The filtration fraction averaged  $22 \pm$   
196  $4\%$  in the leans, and  $23 \pm 5\%$  in the obese, and was not significantly different between the  
197 two groups. In the pooled baseline data, both total renal blood supply and eGFR were

198 directly related to cardiac output, and to each other (**Figure S1**). Data supplements can be  
199 found here: <https://doi.org/10.6084/m9.figshare.9763955>

200

201 *FFA uptake* In the respective selected ROIs, fatty acid uptake was higher in the medulla than  
202 in the cortex ( $p < 0.0001$ ), the two rates being highly correlated with each other ( $r = 0.96$ ,  $p < 0.0001$ ).  
203 Both cortical and medullary fatty acid uptake were higher in obese as compared to lean participants  
204 ( $p = 0.001$  and  $p = 0.0008$ , respectively). When fatty acid uptake is expressed as a fraction of fatty  
205 acid delivery to tissue, uptake remained significantly higher ( $p = 0.01$ ) only in the medulla (**Table 3**).  
206 Renal fatty acid uptake was well correlated with whole-body fat oxidation both in the cortex and the  
207 medulla (**Figure 2**).

208 In addition to plasma FFA and glycerol, obese participants were also characterized by raised  
209 circulating levels of branched-chain amino acids (BCAA), lactate, pyruvate, and citrate (Table 1).  
210 In the pooled baseline data, the  $\beta$ -OH/AcAc ratio was positively associated with both cortical and  
211 medullary FA uptake (**Figure 3**) as well as with whole-body fat oxidation ( $r = 0.37$ ,  $p = 0.025$ ).

212 *Effects of bariatric surgery* Six months following bariatric surgery, participants had lost  $26 \pm$   
213 8 kg, without any difference between RYGB and sleeve gastrectomy (data not shown). Along with  
214 HbA<sub>1c</sub>, circulating concentrations of BCAA, glycerol and pyruvate, but not FFA or ketones, were  
215 all decreased (**Table 1**). Plasma insulin concentrations tended to decrease and insulin sensitivity (as  
216 indexed by OGIS) significantly improved. Cardiac output, gas exchange rates, and energy  
217 expenditure decreased, and there was a trend for whole body fat oxidation also to be reduced (Table  
218 2). Renal volume was decreased while tissue density was increased ( $p = 0.0001$  for both), and eGFR  
219 was reduced. In contrast, perfusion (per unit volume) was unchanged, and neither cortical nor  
220 medullary FA uptake was significantly reduced, either as absolute values or as a fraction of FFA  
221 delivery to the kidneys. When accounting for renal volume, total renal blood flow was decreased  
222 (885 [317] vs 760[367],  $p = 0.006$ ). No difference was seen between RYGB and sleeve gastrectomy  
223 also regarding the change in renal volume, tissue density, or total renal flow (data not shown).

224

## 225 **Discussion**

226

227 The simultaneous measurement of systemic and renal hemodynamics parameters and FFA  
228 uptake in this study yielded several main findings. Firstly, renal volume was increased in the obese,  
229 in keeping with the results of Rea *et al.*(31), who reported larger glomerular planar surface areas in  
230 obese as compared to lean kidney donors (total renal volume was not measured). In our study, the  
231 lower radiodensity in the obese suggests that the nephromegaly might be due to an increase in the

232 water/lipid component. Studies in both animals and humans have demonstrated fat accumulation in  
233 the renal sinus and renal parenchyma. Fat accumulation in the renal sinus is of special interest,  
234 since it may lead to compression of the renal vein and lymphatic vessels, which in turn result in  
235 increases in renal interstitial pressure (27). Obese rabbits with larger fat deposits within the renal  
236 sinus exhibit larger kidneys (7). In humans a ‘‘fatty kidney’’ – or the renal sinus fat volume – has  
237 been shown to associate with a higher risk of hypertension (8) and with the number of prescribed  
238 antihypertensive medications (3). Importantly, in the present study the decrease in renal  
239 radiodensity was almost completely reversed following weight loss over a 6-month time period  
240 (**Table 2**). Taken together, our data indicate that after bariatric surgery any fat accumulation within  
241 the renal parenchyma or renal edema (or combination of the two) can regress to quasi-normal  
242 levels.

243 Secondly, in the obese renal perfusion (per unit tissue mass) was maintained at the level of the  
244 nonobese participants, but their total renal blood flow was higher. Both total eGFR and total blood  
245 flow were increased in proportion to cardiac output (**Table 3 and Figure S1**). In a large biopsy  
246 study of living kidney donors (5), obesity was independently associated with a higher single-  
247 nephron GFR but a normal number of nephrons. Importantly, weight loss reduced the increases in  
248 eGFR, and total blood flow, thereby attenuating the risk of long-term hyperperfusion and kidney  
249 damage.

250 Thirdly, fatty acid uptake was increased in the obese by ~50% in both cortical and medullary  
251 ROIs. [<sup>18</sup>F]-FTHA, *i.e.*, a long-chain fatty acid analogue, undergoes partial metabolism in  
252 mitochondria and is then trapped. Tissue accumulation of [<sup>18</sup>F]-FTHA includes both storage and  
253 oxidation of FFA (18). Of note, since FTHA (like fatty acids) is tightly bound to plasma albumin, it  
254 is not filtered by the glomeruli but is extracted from plasma at the basolateral membrane of tubular  
255 cells. From our data it can be calculated that in obese participants the kidneys extract an average 66  
256  $\mu\text{mol/L}$ , or 8.3%, of the FFA concentration in perfusing plasma. This estimate is in keeping with  
257 the data of Owen *et al.* (28), who used renal catheterization to measure renal FFA extraction  
258 (averaging 85  $\mu\text{mol/L}$ ) in a small group of obese individuals. The very good agreement between  
259 the two studies supports the use of [<sup>18</sup>F]-FTHA-PET to measure FFA uptake *in vivo* non-invasively.  
260 In terms of the intrinsic ability of renal tissue to extract FFA from the plasma (*i.e.*, the fractional  
261 uptake parameter, FUR, **Table 3**), obesity was not associated with an enhanced avidity for this  
262 substrate (especially in the cortex), and the increased FFA uptake was almost entirely the result of  
263 increased delivery of the substrate. The direct correlation between renal FFA uptake and whole-  
264 body fat oxidation (**Figure 3**) supports the interpretation that the kidneys share with other organs  
265 and tissues the increased exposure to fatty substrates resulting from unrestrained lipolysis (4, 16).



266 To the extent that the  $\beta$ -OH/AcAc ratio reflects the mitochondrial redox state (21), its positive  
267 association with renal FFA uptake (**Figure 4**) as well as with whole-body fat oxidation suggests that  
268 the higher renal FFA uptake in the obese induced a higher oxidation of these substrates. In this  
269 context, the raised circulating levels of citrate, lactate, and pyruvate can be regarded as markers of  
270 mitochondrial overload (30).

271 Finally, surgically induced weight loss led to only an attenuation of renal FFA uptake. As  
272 plasma FFA also did not return to the level of nonobese participants, this finding indicates that 6  
273 months after surgery the obese participants were still in a state of negative energy balance and  
274 increased lipolysis. Of note is that the presence of well-controlled, uncomplicated T2D in the obese  
275 group was not associated with any difference in the measured hemodynamic and metabolic  
276 parameters. However, we cannot rule out that more severe hyperglycemia may impact renal  
277 hemodynamics and FFA handling above and beyond the effect of surgery.

278 In previous studies using the PET methodology in obese and nonobese individuals, we have  
279 quantified FFA uptake in liver, subcutaneous and visceral adipose tissue, and skeletal muscle (4, 16,  
280 38). It is of interest to compare FFA uptake across different tissues. Per unit tissue mass, renal  
281 FFA uptake is much larger than in abdominal subcutaneous ( $0.28 \mu\text{mol}\cdot\text{min}^{-1}\cdot 100\text{g}^{-1}$ ) or visceral  
282 adipose tissue ( $0.57 \mu\text{mol}\cdot\text{min}^{-1}\cdot 100\text{g}^{-1}$ ) or resting skeletal muscle ( $0.36 \mu\text{mol}\cdot\text{min}^{-1}\cdot 100\text{g}^{-1}$ ), but only  
283 about half that of liver ( $10.4 \mu\text{mol}\cdot\text{min}^{-1}\cdot 100\text{g}^{-1}$ ). By multiplying tissue uptake rates by the  
284 respective total mass, the contribution of muscle is similar to that of the liver and higher than either  
285 kidney or adipose tissue (**Figure 4**). Of note, the sum of fat uptake rates by these organs averages  $3$   
286  $\mu\text{mol}\cdot\text{min}^{-1}\cdot\text{kg}^{-1}$ , an estimate well within the range of values for FFA turnover obtained with the use  
287 of tracers of oleate or palmitate (11).

288 Our study has limitations. Firstly, GFR was estimated and not directly measured, which  
289 precludes a reliable estimation of intraglomerular pressure and afferent and efferent arteriolar  
290 resistance (*e.g.*, by applying Gomez formula (9)). Secondly, the resolution of the PET/CT scanner  
291 we used does not delineate a clear separation between cortex and medulla. Therefore, ROIs had to  
292 be drawn based on the anatomical references: a thin band of voxels into consecutive planes for the  
293 cortex just underneath the renal capsule and a parallel inner band for the medulla were used. When  
294 anatomically small structures are analyzed, the partial volume and the spillover effect may give rise  
295 to some underestimation and overestimation of the values, respectively. Radiowater is freely  
296 diffusible in and out of cells and thus measures true tissue perfusion. However, it was not possible  
297 to take into account the traffic of water within the kidney medulla and urinary excretion; this  
298 methodological aspect and the adequacy of the arterial input function need further study.  
299 Furthermore, as shown in Figure 1, perfusion in the cortex does not seem homogeneous. The

300 potential heterogeneity in glomerular blood flow and filtration in different nephron populations,  
301 especially between cortical and juxtamedullary nephrons, has been remarked in the past (37). Also,  
302 the physics of positron emission, such as partial volume effects and spillover, may give rise to some  
303 overestimation of medullary perfusion. PET and cardiac MRI measurements were not obtained  
304 simultaneously, so cardiac output may have changed slightly during the PET scan. Finally, the  
305 current study included only women, due to the difficulty in our Center in recruiting morbidly obese  
306 men. Whereas inclusion of both genders would have been more representative of the general  
307 population, our data on renal FFA uptake and perfusion are in close agreement with those of other  
308 studies that have included subjects of both genders (17, 28).

309 In conclusion, our study demonstrates that obesity leads to structural, metabolic and  
310 hemodynamic renal changes. More specifically, in the obese renal volume, FFA uptake and total  
311 renal perfusion are higher as compared to lean participants. After bariatric surgery, total renal  
312 blood flow, and eGFR are decreased, thereby attenuating the risk for progression of obesity-induced  
313 chronic kidney disease. On the contrary, 6 months after bariatric surgery renal FFA uptake is not  
314 normalized.

315

316

317 **Acknowledgments**

318 The authors thank the staff of the Turku PET Centre for performing the PET imaging. The authors  
319 also thank Sauli Piirola for his assistance in Carimas analysis.

320 **Funding.** The current study was conducted within the Center of Excellence into Cardiovascular and  
321 Metabolic Diseases supported by the Academy of Finland (307402), University of Turku, Abo  
322 Akademi University, University of Eastern Finland and Turku University Hospital; Finnish Diabetes  
323 Foundation.

324 **Duality of interest.** No potential conflicts of interest relevant to this article were reported.

325 **Author contributions.** E. R., P.D., V.O., H.I., E.F. analyzed data and literature and drafted the  
326 manuscript. J.C.H conducted the clinical PET studies. P.I., P.N. conceived the study design. E.F.,  
327 P.N. reviewed the manuscript. All authors approved the final version of the manuscript. E.F. and  
328 P.N. are the guarantors of this work and, as such, had full access to all the data in the study and take  
329 responsibility for the integrity of the data and the accuracy of the data analysis.

330

331

332 **References**

333

- 334 1. Report of the expert committee on the diagnosis and classification of diabetes mellitus.  
335 *Diabetes Care* 26 Suppl 1: S5-20, 2003. doi:[10.2337/diacare.26.2007.s5](https://doi.org/10.2337/diacare.26.2007.s5)
- 336 2. **Balaban RS, and Mandel LJ.** Metabolic substrate utilization by rabbit proximal tubule. An  
337 NADH fluorescence study. *Am J Physiol* 254: F407-416, 1988. doi: [10.1152/ajprenal.1988.254.3.F407](https://doi.org/10.1152/ajprenal.1988.254.3.F407)
- 338 3. **Chughtai HL, Morgan TM, Rocco M, Stacey B, Brinkley TE, Ding J, Nicklas B, Hamilton C, and**  
339 **Hundley WG.** Renal sinus fat and poor blood pressure control in middle-aged and elderly individuals at risk  
340 for cardiovascular events. *Hypertension* 56: 901-906, 2010. doi: [10.1161/HYPERTENSIONAHA.110.157370](https://doi.org/10.1161/HYPERTENSIONAHA.110.157370)
- 341 4. **Dadson P, Ferrannini E, Landini L, Hannukainen JC, Kalliokoski KK, Vaittinen M, Honka H,**  
342 **Karlsson HK, Tuulari JJ, Soinio M, Salminen P, Parkkola R, Pihlajamaki J, Iozzo P, and Nuutila P.** Fatty acid  
343 uptake and blood flow in adipose tissue compartments of morbidly obese subjects with or without type 2  
344 diabetes: effects of bariatric surgery. *Am J Physiol Endocrinol Metab* 313: E175-e182, 2017. doi:  
345 [10.1152/ajpendo.00044.2017](https://doi.org/10.1152/ajpendo.00044.2017)
- 346 5. **Denic A, Mathew J, Lerman LO, Lieske JC, Larson JJ, Alexander MP, Poggio E, Glassock RJ,**  
347 **and Rule AD.** Single-Nephron Glomerular Filtration Rate in Healthy Adults. *N Engl J Med* 376: 2349-2357,  
348 2017. doi: [10.1056/NEJMoa1614329](https://doi.org/10.1056/NEJMoa1614329)
- 349 6. **Du Bois D, and Du Bois EF.** A formula to estimate the approximate surface area if height and  
350 weight be known. 1916. *Nutrition* 5: 303-311; discussion 312-3, 1989.
- 351
- 352 7. **Dwyer TM, Banks SA, Alonso-Galicia M, Cockrell K, Carroll JF, Bigler SA, and Hall JE.**  
353 Distribution of renal medullary hyaluronan in lean and obese rabbits. *Kidney Int* 58: 721-729, 2000. doi:  
354 [10.1046/j.1523-1755.2000.00218.x](https://doi.org/10.1046/j.1523-1755.2000.00218.x)
- 355 8. **Foster MC, Hwang SJ, Porter SA, Massaro JM, Hoffmann U, and Fox CS.** Fatty kidney,  
356 hypertension, and chronic kidney disease: the Framingham Heart Study. *Hypertension* 58: 784-790, 2011.  
357 doi: [10.1161/HYPERTENSIONAHA.111.175315](https://doi.org/10.1161/HYPERTENSIONAHA.111.175315)
- 358 9. **Gomez DM.** Evaluation of renal resistances, with special reference to changes in essential  
359 hypertension. *J Clin Invest* 30: 1143-1155, 1951. doi: [10.1172/JCI102534](https://doi.org/10.1172/JCI102534)
- 360 10. **Gruner JM, Paamand R, Hojgaard L, and Law I.** Brain perfusion CT compared with 15O-H2O-  
361 PET in healthy subjects. *EJNMMI Res* 1: 28, 2011. doi: [10.1186/2191-219X-1-28](https://doi.org/10.1186/2191-219X-1-28)
- 362 11. **Han Q, Cao Y, Gathaiya N, Kemp BJ, and Jensen MD.** Free fatty acid flux measured using [1-  
363 (11)C]palmitate positron emission tomography and [U-(13)C]palmitate in humans. *Am J Physiol Endocrinol*  
364 *Metab* 314: E413-e417, 2018. doi: [10.1152/ajpendo.00284.2017](https://doi.org/10.1152/ajpendo.00284.2017)
- 365 12. **Haroun MK, Jaar BG, Hoffman SC, Comstock GW, Klag MJ, and Coresh J.** Risk factors for  
366 chronic kidney disease: a prospective study of 23,534 men and women in Washington County, Maryland. *J*  
367 *Am Soc Nephrol* 14: 2934-2941, 2003. doi: [10.1097/01.asn.0000095249.99803.85](https://doi.org/10.1097/01.asn.0000095249.99803.85)
- 368 13. **Helmio M, Victorzon M, Ovaska J, Leivonen M, Juuti A, Jaser N, Peromaa P, Tolonen P,**  
369 **Hurme S, and Salminen P.** SLEEVEPASS: a randomized prospective multicenter study comparing  
370 laparoscopic sleeve gastrectomy and gastric bypass in the treatment of morbid obesity: preliminary results.  
371 *Surg Endosc* 26: 2521-2526, 2012. doi: [10.1007/s00464-012-2225-4](https://doi.org/10.1007/s00464-012-2225-4)

- 372 14. **Honka H, Koffert J, Hannukainen JC, Tuulari JJ, Karlsson HK, Immonen H, Oikonen V,**  
373 **Tolvanen T, Soinio M, Salminen P, Kudomi N, Mari A, Iozzo P, and Nuutila P.** The effects of bariatric  
374 surgery on pancreatic lipid metabolism and blood flow. *J Clin Endocrinol Metab* 100: 2015-2023, 2015. doi:  
375 [10.1210/jc.2014-4236](https://doi.org/10.1210/jc.2014-4236)
- 376 15. **Hovik R, Osmundsen H, Berge R, Aarsland A, Bergseth S, and Bremer J.** Effects of thia-  
377 substituted fatty acids on mitochondrial and peroxisomal beta-oxidation. Studies in vivo and in vitro.  
378 *Biochem J* 270: 167-173, 1990. doi: [10.1042/bj2700167](https://doi.org/10.1042/bj2700167)
- 379 16. **Immonen H, Hannukainen JC, Kudomi N, Pihljamäki J, Saunavaara V, Laine J, Salminen P,**  
380 **Lehtimäki T, Pham T, Iozzo P, Nuutila P.** Increased Liver Fatty Acid Uptake Is Partly Reversed and Liver Fat  
381 Content Normalized After Bariatric Surgery. *Diabetes Care* 41: 368-371, 2018. doi: [10.2337/dc17-0738](https://doi.org/10.2337/dc17-0738)
- 382 17. **Inaba T, Yamashita M, Kawase Y, Nakahashi H, and Watanabe H.** Quantitative  
383 measurement of renal plasma flow by positron emission tomography with oxygen-15 water. *Tohoku J Exp*  
384 *Med* 159: 283-289, 1989. doi: [10.1620/tjem.159.283](https://doi.org/10.1620/tjem.159.283)
- 385 18. **Karmi A, Iozzo P, Viljanen A, Hirvonen J, Fielding BA, Virtanen K, Oikonen V, Kempainen J,**  
386 **Viljanen T, Guiducci L, Haaparanta-Solin M, Nagren K, Solin O, and Nuutila P.** Increased brain fatty acid  
387 uptake in metabolic syndrome. *Diabetes* 59: 2171-2177, 2010. doi: [10.2337/db09-0138](https://doi.org/10.2337/db09-0138)
- 388 19. **Kopelman PG.** Obesity as a medical problem. *Nature* 404: 635-643, 2000. doi:  
389 [10.1038/35007508](https://doi.org/10.1038/35007508)
- 390 20. **Koskenvuo JW, Karra H, Lehtinen J, Niemi P, Parkka J, Knuuti J, and Hartiala JJ.** Cardiac MRI:  
391 accuracy of simultaneous measurement of left and right ventricular parameters using three different  
392 sequences. *Clin Physiol Funct Imaging* 27: 385-393, 2007. doi: [10.1111/j.1475-097X.2007.00764.x](https://doi.org/10.1111/j.1475-097X.2007.00764.x)
- 393 21. **Krebs HA, and Gascoyne T.** The redox state of the nicotinamide-adenine dinucleotides in rat  
394 liver homogenates. *Biochem J* 108: 513-520, 1968. doi: [10.1042/bj1080513](https://doi.org/10.1042/bj1080513)
- 395 22. **Kudomi N, Koivuviita N, Liukko KE, Oikonen VJ, Tolvanen T, Iida H, Tertti R, Metsarinne K,**  
396 **Iozzo P, and Nuutila P.** Parametric renal blood flow imaging using [15O]H<sub>2</sub>O and PET. *Eur J Nucl Med Mol*  
397 *Imaging* 36: 683-691, 2009. doi: [10.1007/s00259-008-0994-8](https://doi.org/10.1007/s00259-008-0994-8)
- 398 23. **Levey AS, Stevens LA, Schmid CH, Zhang YL, Castro AF, 3rd, Feldman HI, Kusek JW, Eggers P,**  
399 **Van Lente F, Greene T, and Coresh J.** A new equation to estimate glomerular filtration rate. *Annals of*  
400 *internal medicine* 150: 604-612, 2009. doi: [10.1093/ndt/gfs529](https://doi.org/10.1093/ndt/gfs529)
- 401 24. **Luaces M, Martinez-Martinez E, Medina M, Miana M, Gonzalez N, Fernandez-Perez C, and**  
402 **Cachafeiro V.** The impact of bariatric surgery on renal and cardiac functions in morbidly obese patients.  
403 *Nephrol Dial Transplant* 27 Suppl 4: iv53-57, 2012. doi: [10.1093/ndt/gfs529](https://doi.org/10.1093/ndt/gfs529)
- 404 25. **Mari A, Pacini G, Murphy E, Ludvik B, and Nolan JJ.** A model-based method for assessing  
405 insulin sensitivity from the oral glucose tolerance test. *Diabetes Care* 24: 539-548, 2001. doi:  
406 [10.2337/diacare.24.3.539](https://doi.org/10.2337/diacare.24.3.539)
- 407 26. **Meury L, Noel J, Tejedor A, Senecal J, Gougoux A, and Vinay P.** Glucose metabolism in dog  
408 inner medullary collecting ducts. *Ren Physiol Biochem* 17: 246-266, 1994. doi: [10.1159/000173829](https://doi.org/10.1159/000173829)
- 409  
410 27. **Ott CE, Navar LG, and Guyton AC.** Pressures in static and dynamic states from capsules  
411 implanted in the kidney. *Am J Physiol* 221: 394-400, 1971. doi: [10.1152/ajplegacy.1971.221.2.394](https://doi.org/10.1152/ajplegacy.1971.221.2.394)
- 412 28. **Owen OE, Felig P, Morgan AP, Wahren J, and Cahill GF, Jr.** Liver and kidney metabolism  
413 during prolonged starvation. *J Clin Invest* 48: 574-583, 1969. doi: [10.1172/JCI106016](https://doi.org/10.1172/JCI106016)

- 414 29. **Patlak CS, and Blasberg RG.** Graphical evaluation of blood-to-brain transfer constants from  
415 multiple-time uptake data. Generalizations. *J Cereb Blood Flow Metab* 5: 584-590, 1985. doi:  
416 [10.1038/jcbfm.1985.87](https://doi.org/10.1038/jcbfm.1985.87)
- 417 30. **Randle PJ, Garland PB, Hales CN, and Newsholme EA.** The glucose fatty-acid cycle. Its role in  
418 insulin sensitivity and the metabolic disturbances of diabetes mellitus. *Lancet* 1: 785-789, 1963. doi:  
419 [10.1016/s0140-6736\(63\)91500-9](https://doi.org/10.1016/s0140-6736(63)91500-9)
- 420 31. **Rea DJ, Heimbach JK, Grande JP, Textor SC, Taler SJ, Prieto M, Larson TS, Cosio FG, and**  
421 **Stegall MD.** Glomerular volume and renal histology in obese and non-obese living kidney donors. *Kidney Int*  
422 70: 1636-1641, 2006. doi: [10.1038/sj.ki.5001799](https://doi.org/10.1038/sj.ki.5001799)
- 423 32. **Rose BD, Post TW, Narins R, and Post T.** *Clinical Physiology of Acid-Base and Electrolyte*  
424 *Disorders*. New York: McGraw-Hill Education, 2001.
- 425  
426 33. **Schmid H, Scholz M, Mall A, Schmidt U, Guder WG, and Dubach UC.** Carbohydrate  
427 metabolism in rat kidney: heterogeneous distribution of glycolytic and gluconeogenic key enzymes. *Curr*  
428 *Probl Clin Biochem* 8: 282-289, 1977.
- 429  
430 34. **Schrauwen P, Wagenmakers AJ, van Marken Lichtenbelt WD, Saris WH, and Westerterp**  
431 **KR.** Increase in fat oxidation on a high-fat diet is accompanied by an increase in triglyceride-derived fatty  
432 acid oxidation. *Diabetes* 49: 640-646, 2000. doi: [10.2337/diabetes.49.4.640](https://doi.org/10.2337/diabetes.49.4.640)
- 433 35. **Silva P.** Energy and fuel substrate metabolism in the kidney. *Semin Nephrol* 10: 432-444,  
434 1990.
- 435  
436 36. **Soininen P, Kangas AJ, Wurtz P, Suna T, and Ala-Korpela M.** Quantitative serum nuclear  
437 magnetic resonance metabolomics in cardiovascular epidemiology and genetics. *Circ Cardiovasc Genet* 8:  
438 192-206, 2015. doi: [10.1161/CIRCGENETICS.114.000216](https://doi.org/10.1161/CIRCGENETICS.114.000216)
- 439 37. **Steinhausen M, Endlich K, and Wiegman DL.** Glomerular blood flow. *Kidney Int* 38: 769-784,  
440 1990. doi: [10.1038/ki.1990.271](https://doi.org/10.1038/ki.1990.271)
- 441 38. **Turpeinen AK, Takala TO, Nuutila P, Axelin T, Luotolahti M, Haaparanta M, Bergman J,**  
442 **Hamalainen H, Iida H, Maki M, Uusitupa MI, and Knuuti J.** Impaired free fatty acid uptake in skeletal  
443 muscle but not in myocardium in patients with impaired glucose tolerance: studies with PET and 14(R,S)-  
444 [18F]fluoro-6-thia-heptadecanoic acid. *Diabetes* 48: 1245-1250, 1999. doi: [10.2337/diabetes.48.6.1245](https://doi.org/10.2337/diabetes.48.6.1245)
- 445 39. **Wang Y, Chen X, Song Y, Caballero B, and Cheskin LJ.** Association between obesity and  
446 kidney disease: a systematic review and meta-analysis. *Kidney Int* 73: 19-33, 2008. doi:  
447 [10.1038/sj.ki.5002586](https://doi.org/10.1038/sj.ki.5002586)
- 448 40. **World Health O.** *Obesity and overweight*. Geneva: World Health Organization, 2018.
- 449

450

451

452 **Figure legends**

453

454 **Figure 1** – Region of interest (ROI) placement in the renal cortex and medulla in a [ $^{15}\text{O}$ ]- $\text{H}_2\text{O}$   
455 image (A) and an [ $^{18}\text{F}$ ]-FTHA image (B). (C): Volume of interest depicting how renal volume was  
456 measured.

457 **Figure 2** – In the whole dataset, whole-body fat oxidation correlated positively with cortical (A)  
458 and medullary FFA uptake (B).

459 **Figure 3** –  $\beta\text{-OH}/\text{AcAC}$ , a surrogate of the mitochondrial  $\text{NAD}^+/\text{NADH}$  balance, correlated  
460 positively both with cortical (A) and medullary FFA uptake (B).  $\beta\text{-OH}$ :  $\beta\text{-OH}$ -butyrate; AcAC:  
461 acetoacetate.

462 **Figure 4** – FFA uptake in several tissues measured in the same subjects. Whereas renal FFA  
463 uptake per unit tissue mass is only second to hepatic FFA uptake, when accounting for the tissue  
464 mass renal FFA uptake is similar to those of fat depots. In all tissues FFA uptake was higher in the  
465 obese as compared to the lean controls. SC: abdominal subcutaneous fat, VF: visceral fat, SM:  
466 skeletal muscle. Entries are mean $\pm$ SE.

467

**Table 1 - Clinical and metabolic characteristics of the 2 study groups §**

	Controls (n = 15)	Obese (n = 23)		p <sup>o</sup>
		Before	After	
Age (years)	45 ± 12	43 ± 10	-	-
BMI (kg/m <sup>2</sup> )	22.6 ± 2.8	41.1 ± 4.2*	31.8 ± 4.2#	<0.0001
WHR (cm/cm)	0.77 ± 0.05	0.89 ± 0.07*	0.87 ± 0.09#	0.04
Fat mass (kg)	19 ± 6	56 ± 10*	37 ± 9#	<0.0001
Fat-free mass (kg)	42 ± 4	56 ± 9*	49 ± 6#	<0.0001
eGFR (mL min <sup>-1</sup> ·1.73 m <sup>-2</sup> )	107 ± 10	103 ± 14	105 ± 17	ns
Systolic BP (mmHg)	128 ± 16	130 ± 15	127 ± 14	ns
Diastolic BP (mmHg)	78 ± 9	85 ± 10	80 ± 11	0.04
TG (mmol·L <sup>-1</sup> )	0.66 ± 0.32	1.18 ± 0.42*	1.09 ± 0.54#	ns
Glucose (mmol·L <sup>-1</sup> )	5.13 ± 0.34	5.71 ± 1.03*	5.30 ± 0.79	ns
Insulin (μU·mL <sup>-1</sup> )	3.0 [3.5]	9.5 [10.8]*	4.0 [3.0]	(0.06)
OGIS (ml·min <sup>-1</sup> ·m <sup>-2</sup> )	426 [91]	351 [67] *	444 [63]	<0.0001
HbA <sub>1c</sub> (%), (mmol/mol)	5.6±0.3, (38±3)	6.0±0.7, (42±7)*	5.4±0.4, (36±5)	<0.0001
FFA (mmol·L <sup>-1</sup> )	0.55 ± 0.17	0.80 ± 0.22*	0.77 ± 0.17#	ns
Glycerol (μmol/L)	67 ± 23	113 ± 31*	108 ± 53#	0.01
BCCA (μmol/L)	250 ± 45	294 ± 42*	241 ± 48	<0.0001
β-OH-butyrate (μmol/L)	110 [180]	140 [140]	188 [218]	ns
Acetoacetate (μmol/L)	36 [49]	44 [34]	55 [36]	ns
Lactate (μmol/L)	1186 ± 182	1460 ± 322*	1337 ± 226#	ns
Pyruvate (μmol/L)	72 ± 18	88 ± 25*	78 ± 25	0.046
Citrate (μmol/L)	110 [22]	125 [33]*	127 [29]#	ns

§ Data are mean ± SD or median [IQR]; BCAA= branched-chained amino acids; \* p≤0.05 obese vs controls; ° after vs before surgery; # p ≤0.05 obese after surgery vs controls.



**Table 2 – Whole-body parameters.<sup>§</sup>**

	Controls	Obese		<i>p</i> <sup>°</sup>
		Before	After	
Cardiac output (CO) (L·min <sup>-1</sup> )	5.2 [1.2]	6.5 [2.8]*	5.9 [1.9]#	0.0019
Cardiac index (L·min <sup>-1</sup> ·m <sup>-2</sup> )	3.11 [0.61]	3.01 [1.07]	3.11 [0.76]	ns
Heart rate (bpm)	59 ± 11	59 ± 10	56 ± 8	ns
VO <sub>2</sub> (mL·min <sup>-1</sup> )	185 ± 18	259 ± 30*	230 ± 34#	<0.0001
VO <sub>2</sub> (mL·min <sup>-1</sup> ·kg <sub>FFM</sub> <sup>-1</sup> )	4.4 ± 0.4	4.7 ± 0.4	4.7 ± 0.5	ns
VCO <sub>2</sub> (mL·min <sup>-1</sup> )	155 ± 15	212 ± 26*	192 ± 33#	0.001
VCO <sub>2</sub> (mL·min <sup>-1</sup> ·kg <sub>FFM</sub> <sup>-1</sup> )	3.7 ± 0.3	3.8 ± 0.34	3.9 ± 0.6	ns
Fat oxidation (μmol·min <sup>-1</sup> )	59 ± 18	89 ± 26*	76 ± 35#	(0.06)
CHO oxidation (μmol·min <sup>-1</sup> )	611 ± 199	771 ± 297*	755 ± 441#	ns
Energy expenditure (kcal·day <sup>-1</sup> )	1299 ± 122	1807 ± 212*	1614 ± 240#	<0.0001

<sup>§</sup>Data are mean ± SD or median [IQR]; VO<sub>2</sub> = oxygen consumption; VCO<sub>2</sub> = carbon dioxide production; CHO = carbohydrate; \* *p* ≤ 0.05 obese vs controls; ° after vs before surgery; # *p* ≤ 0.05 obese after surgery vs controls.

**Table 3 – Renal parameters.<sup>§</sup>**

	Controls	Obese		<i>p</i> <sup>°</sup>
		Before	After	
Renal volume (mL)	256 [63]	340 [118]*	310 [118]#	0.0001
Radiodensity (HU)	31.5 [9.8]	15.3 [13.1]*	26.9 [9.0]	<0.0001
Cortical blood perfusion (mL·min <sup>-1</sup> ·100mL <sup>-1</sup> )	268 [104]	262 [62]	246 [62]	ns
Medullary blood perfusion (mL·min <sup>-1</sup> ·100mL <sup>-1</sup> )	163 [72]	149 [51]	166 [53]	ns
Total renal BF (mL·min <sup>-1</sup> )	749 [300]	885 [317]*	760 [367]	0.006
Renal BF/CO (%)	16 ± 4	15 ± 4	15 ± 6	ns
eGFR (mL/min)	104 ± 11	129 ± 23*	118 ± 24#	0.0025
Hematocrit (%)	36.6 ± 2.7	39.5 ± 2.2*	38.3 ± 3.7	(<0.1)
Filtration fraction (%)	22 ± 4	23 ± 5	24 ± 5	ns
Cortical FAU (μmol·min <sup>-1</sup> ·100g <sup>-1</sup> )	4.1 ± 1.5	6.3 ± 1.8*	6.0 ± 1.8#	ns
Cortical FUR (%)	7.7 ± 1.2	8.2 ± 1.3	8.1 ± 1.9	ns
Medullary FAU (μmol·min <sup>-1</sup> ·100g <sup>-1</sup> )	4.6 ± 2.1	7.5 ± 2.2*	6.9 ± 1.9#	ns
Medullary FUR (%)	8.4 ± 2.1	9.9 ± 1.5*	9.4 ± 1.9	ns

<sup>§</sup>Data are mean ± SD or median [IQR]; BF = blood flow; CO = cardiac output; FUR = fractional FA uptake rate; FAU = FFA uptake; \* *p* ≤ 0.05 obese vs controls; ° after vs before surgery; # *p* ≤ 0.05 obese after surgery vs controls.

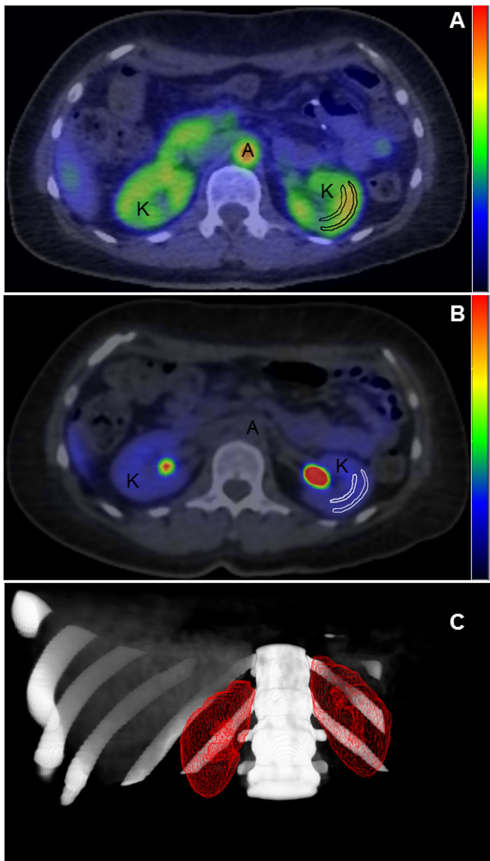
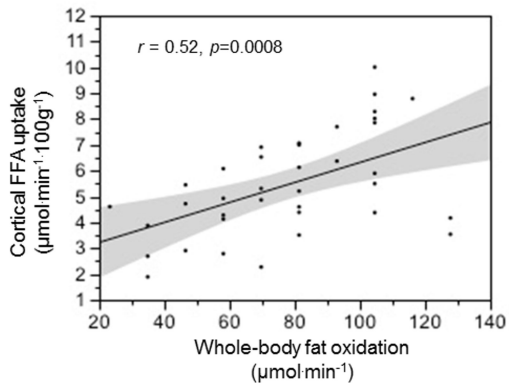


Figure 1

**A.**



**B.**

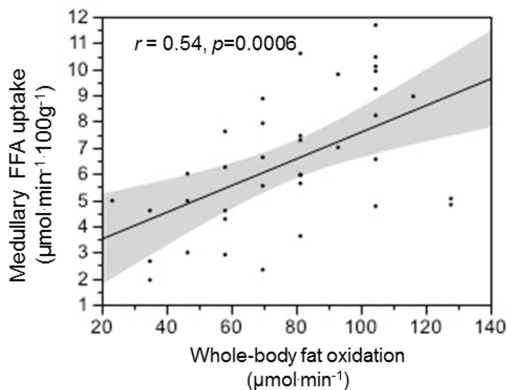
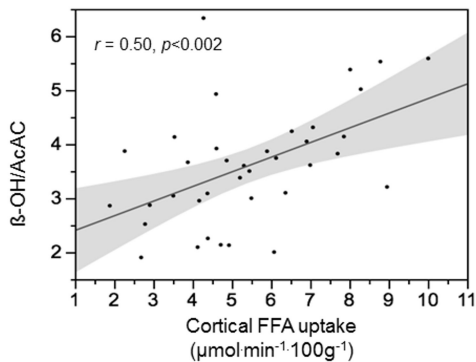


Figure 2

**A.**



**B.**

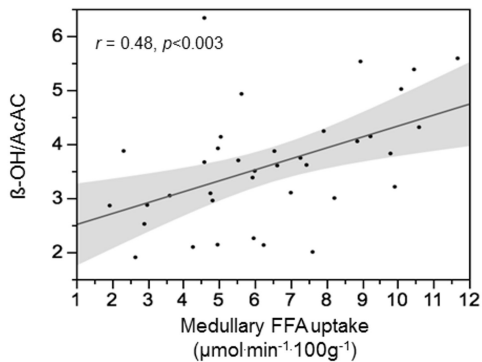


Figure 3

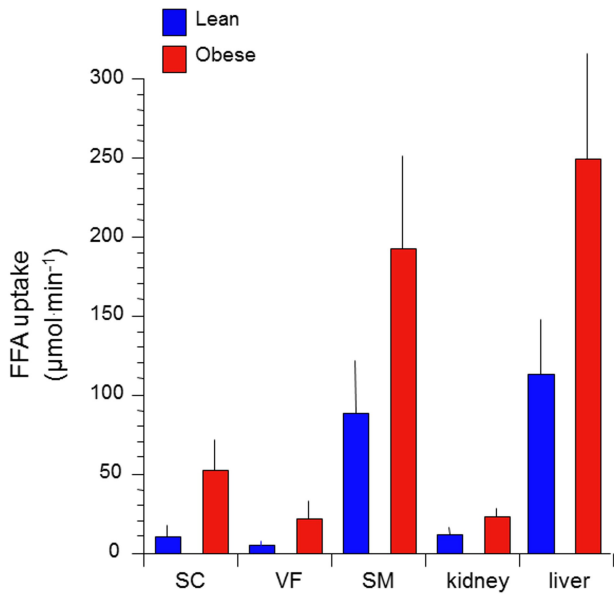


Figure 4